A Tool for Monitoring Piezoelectric Micro-Pumps

J.M. Cittadino and E. Mendes, Laboratoire de Conception et d'Intégration des Systèmes (EA 3747), INPG-ESISAR, Valence, France; A. Soucemarianadin, Laboratoire des Ecoulements Géophysiques et Industriels (UMR 5519), UJF-CNRS-INPG, Grenoble, France

Abstract

Piezoelectric micro-pumps are largely used in drop on demand applications for medical purpose and in the printing industry. In order to diagnose and control such a system, a non-linear model has been developed to predict the velocity of the ejected drop. We show here that data from experiments are in good agreement with our model predictions, showing that the ejection velocity is strong a function of the applied voltage.

Introduction

In the field of microfluidics, many devices such as microscale total analysis systems (µTAS)[1,2] and other specialized systems are being developed presently for genetic analysis[3] or clinical diagnosis.[4] A key component in such a system is the micro-pump which may be fabricated following different techniques.[5,6] Besides these new applications, piezoelectric micro-pumps have always been one of the main components in ink-jet printing systems.[7] In actual printing systems, there may be a large discrepancy between required and measured ejection velocities what is even worse, is that differences in characteristics may occur from one drop to another leading to a loss of quality in the printed patterns.

To remedy to the above cited problems we propose in this paper, a tool which should help to analyze and control the flow for drop on demand applications. We show here that this tool based on a non linear model, is able to predict accurately the ejection velocity of a droplet, the ejected volume and the pinch-off time.

In case of discrepancy between required and measured velocities, i.e. nozzle clogging, the tool is able to control the system acting on the transducer in such a way as to reduce the tracking error (the difference between required and measured velocities), these different steps will be developed in this paper.

System Modeling

Geometrical Configuration

In general, the geometrical configurations of industrial systems may be quite complicated to model or even not fully characterized. For this purpose, an equivalent mechanical system comprising an axisymmetric chamber fitted with a piezoelectric transducer and for which the unknowns are the length and radius of the chamber and the piezoelectric characteristics of the transducer is proposed. This is for the simplest case and one may consider many other unknowns as shown later. The considered equivalent micro-pump comprises the transducer at one end and the nozzle, with a known radius, at the other end. The inlet is connected to the fluid reservoir and the outlet comprising the nozzle, of much smaller dimension than the inner diameter of the chamber,[8] is represented in figure 1.

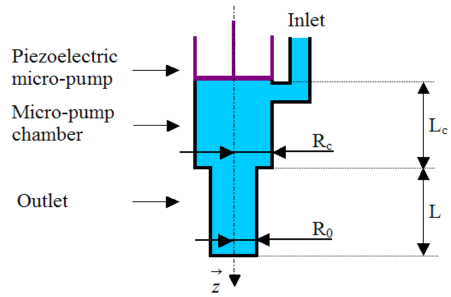

Figure 1. Equivalent mechanical system

Determination of the Flow in the Pipe

The ejection process can be described by the following three steps[8]:

- Displacement of the transducer and consequent transient start-up of the fluid (Step one).
- Backward movement of the transducer when the voltage step is finished (i.e. U=0V) (Step two).
- Drop formation (Step three).
- Drop ejection (Step four).

Is important to notice that in this work, negative voltages are not considered.

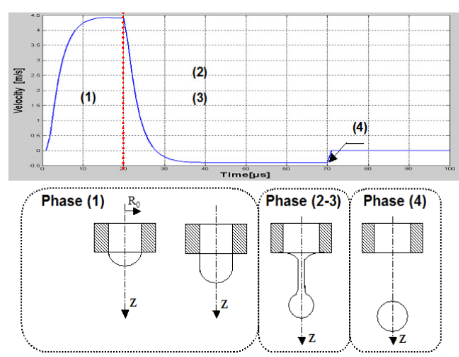

Figure 2. Ejection process

Step One: Transient Start-Up of the Fluid

The fluid is taken to be viscous and Newtonian. Considering the flow in a circular pipe, the velocity in this pipe is given by:

$$\frac{\partial V_z(t,r)}{\partial t} = -\frac{1}{\rho}\frac{\partial P(t,z)}{\partial z} + \frac{\mu}{\rho}\left(\frac{1}{r}\frac{\partial}{\partial r}\left(r \cdot \frac{\partial V_z(t,r)}{\partial r}\right)\right) \tag{1}$$

where Vz(t,r) is the velocity on the axis of the flow, ρ is the fluid density, μ the viscosity of the fluid and P(t,z) the pressure term.

Assuming that the pressure gradient is constant in the pipe, we obtain:

$$\frac{\partial P(t,z)}{\partial z} = -\frac{P(t,z)}{L} = -\frac{P_{pzt}(t,z) - P_{cap}(t) - P_{c\log}(t)}{L} \tag{2}$$

L is the pipe length $P_{pzt}(t,z)$ the pressure created by the transducer, P_{cap} the capillarity back pressure defined by:

$$\begin{cases} P_{cap} = 0 & \text{, if } V_z = 0 \\ P_{cap} = 2\gamma / R_0 & \text{, if } V_z > 0 \end{cases} \tag{3}$$

γ the superficial tension, a singular head loss representing the clogging effect:

$$P_{c\log}(t) = \frac{1}{2}\rho k_{c\log} V_z(t)^2 \tag{4}$$

with $k_{clog} \in \Re^+$.

In order to express the fluid velocity we have to detail the deformation of the piezoelectric transducer.[9]

$$\varepsilon = \frac{\Delta e}{e} = \frac{T_{fluid/pzt}}{E} + \frac{d_{33}U}{e} \tag{5}$$

with E the Young modulus, $T_{fluid/pzt} = -P_{pzt}$ the mechanical stress (equivalent to a pressure term), d_{33} the piezoelectric strain coefficient, U the applied voltage, e the transducer thickness. Considering an incompressible fluid, equation (1) becomes:

$$\frac{\partial V_z(t,r)}{\partial t} = \frac{1}{\rho L}\left(P_{pzt}(t,z) - P_{c\log}(t) - P_{cap}\right) + \frac{\mu}{\rho}\left(\frac{1}{r}\frac{\partial}{\partial r}\left(r\frac{\partial V_z(t,r)}{\partial r}\right)\right) \tag{6}$$

with the following initial and boundary conditions:

$$\begin{cases} V_z\big|_{t=0} = 0 \ \forall \mathrm{r} \in [-R_0 \quad R_0] \\ V_z(R,t) = 0 \ \forall t \end{cases}$$

and

$$\begin{cases} P_{pzt}(t,z) = 0 & \text{, if } \mathrm{U}(\mathrm{t}) = 0. \\ P_{pzt}(t,z) = 0 & \text{, if } \Delta e(t) = \Delta e_{\max}. \\ P_{pzt}(t,z) = E\left[\frac{d_{33}U(t)}{e} - \frac{R_0^2}{eR_c^2}\int_0^t V_z(t')dt'\right] & \text{, if } \Delta e(t) < \Delta e_{\max}. \end{cases} \tag{7}$$

Step Two: Backward Movement of the Transducer

When the transducer returns back to its initial position, this leads to a decrease of the ejection velocity.
Applying Newton's first law:

$$\frac{dV_z(t)}{dt} = -\underbrace{\left(\frac{\frac{2\gamma}{R_0} + P_{atm}}{\rho \cdot L_c}\right)}_{F_1} - \underbrace{\left(\frac{2\gamma R_c}{\rho\cdot\pi\cdot R_0^2 L_c}\right)}_{F_2} + \underbrace{\frac{\mu}{\rho}\left(\frac{1}{r}\frac{\partial}{\partial r}\left(r\cdot\frac{\partial V_z(t,r)}{\partial r}\right)\right)}_{F_3} \tag{8}$$

and with

$$\begin{cases} V_z\big|_{t=0} = 0 \ \forall \mathrm{r} \in [0 \quad R_0] \\ V_z(R_0,t) = 0 \ \forall t \end{cases}$$

F1, accounts for the ambient and capillary pressures whilst the second term, F2, characterizes the interaction between the transducer and the fluid.[10] Finally, the third term, F3, represents the viscous stresses. The weight can be neglected here because it is very small compared to the other forces acting in this case.

Step Three and Four: Drop Formation and Detachment

In the first phase, a volume of fluid is expulsed through the nozzle and this corresponds to the initial volume of the drop, $V_{ol\_drop\_init}$. The velocity of the latter is equal to the maximum of the flow velocity. The drop volume grows much more slowly during the second phase. During the third step, the drop under formation is deformed by the surface tension effect as represented in figures (2,3) and it is possible to determine if a drop is really formed or not (phase four).

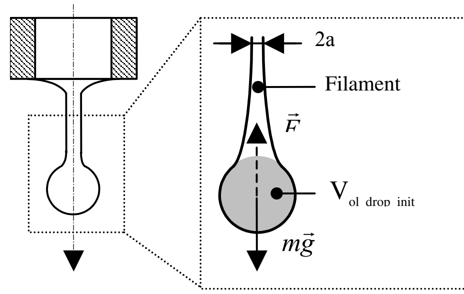

Figure 3. Schematic of drop formation representing the main forces in presence

From the equilibrium of forces, the velocity of the drop which may detach, is given below:

$$\frac{dV_{drop\_fall}(t)}{dt} = \frac{d^2 z_g(t)}{dt^2} = g - \frac{2\pi a(t)\gamma}{\rho V_{ol\_out}(t)} \tag{9}$$

with $V_{drop\_fall}(0) = \max(V_z(t,0))$, a(t) the minimum radius of the filament, z_g the length of the filament and where $F(t)=2\pi a(t)\gamma$ represents the surface tension effect, and V_{ol_out} is the fluid volume expulsed out of the nozzle:

$$V_{ol\_out}(t) = \pi R_0^2 \int_0^t V_z(\tau)\, d\tau \tag{10}$$

A necessary condition for drop detachment is:

$$\frac{dV_{drop\_fall}(t)}{dt} > 0 \tag{11}$$

If the initial volume of the drop is such as the above condition is not fulfilled then the mass of the fluid retracts back into the nozzle and the flow is stopped (i.e. no drop detachment happens).

If this condition is fulfilled, then the drop is ejected and the pinch-off time, T_{poff} is given by:

$$\frac{dV_{drop\_fall}(T_{poff})}{dt} = 0 \tag{12}$$

Moreover the volume of the ejected drop, V_{ol_drop}, is:

$$V_{ol\_drop} = V_{ol\_out}\left(T_{poff}\right) \tag{13}$$

According to figure 4, the evolution of the minimum radius of the filament (a(t)) can be estimated using:

$$\int_0^{z_g(t)} \pi r^2(z)\, dz = V_{ol\_out}(t) - V_{ol\_drop\_init} \tag{14}$$

where r(z) is defined:

$$\begin{cases} r(z) = \dfrac{R_0 - a(t)}{1 - e^{-\frac{\beta}{\delta}}} \cdot \left(e^{-\frac{z}{z_g(t)} \cdot \beta} - 1 \right) + R_0 & , \text{if } z \in \left[0 \quad \dfrac{z_g(t)}{\delta} \right] \\ r(z) = a(t) & , \text{if } z \in \left[\dfrac{z_g(t)}{\delta} \quad z_g(t) \right] \end{cases} \tag{15}$$

and with the following boundary conditions:

$$\begin{cases} r(0) = R_0 \\ r\left(\dfrac{z_g(t)}{\delta} \right) = a(t) \end{cases} \tag{16}$$

where (β, δ) are some real fixed number.

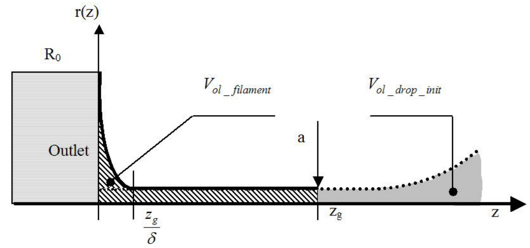

Figure 4. Schematic of the drop profile representing the upstream and downstream curvatures of the drop.

Validation

Model Linearization

In order to solve equations (1,8) the backward algorithm of the finite difference method on the spatial term is used.

This approach can be extended to any geometrical configuration of the micro-pump using either finite differences or finite elements depending on the complexity of the flow geometry. Then, putting it into a matrix form to be solved later using MATLAB®, and for a given number, n, of spatial discretization points, we obtain:

$$\frac{\mu}{\rho} \left(\frac{1}{r} \frac{\partial}{\partial r} \left(r \frac{\partial V_z(t,r)}{\partial r} \right) \right) = \mathbf{A} V_z(t) \tag{17}$$

where $\mathbf{A} \in M_{n,n}$

Experimental Set-Up

The experimental set-up used in this work comprises a droplet generating device, an illumination source, a fast shutter camera and an optical system. The images are acquired and then processed using the "Image processing" toolbox from MATLAB®.

Calibration

For the calibration purpose, we use an industrial print-head for which we know some of the characteristics .The simulation tool is sufficiently robust to take into account various parameters which may influence the behavior of a print-head. Assuming that all unknown geometrical configuration can be transformed into an equivalent form as presented in figure 1, unknown parameters can be identified to predict the behavior of such a device.

Table 1: Comparison between theoretical and experimental values after calibration for a Spectra® print-head

	Initial volume (L)	Velocity (L)	Ejected volume (L)	Pinch off
Theoretical	$3.01.10^{-11}$ L	4.39 $m.s^{-1}$	$3.02.10^{-11}$ L	73 µs
Experimental	3.10^{-11} L	4.4 $m.s^{-1}$	$2.99.10^{-11}$ L	73 µs

Design of a Control System

The present work is focused on the adaptative control of the voltage level applied to the transducer during the first step of the ejection process. The control of the velocity of the ejected drop at the end of step one is of primary importance. Indeed if the flow is constant for a fixed time, the ejected volume will be constant too.

Model Simplification

Equation (6) is quite complicated in the view of the establishment of the control strategy. Taking into account the fact that in a cylindrical pipe, the velocity profile in the radius direction is parabolic:

$$\mathbf{V}_z\left(t,r\right)=\mathbf{V}_z\left(t,r=0\right)\left(1-\frac{r^2}{R_0^2}\right)=\mathbf{V}\left(t\right)\left(1-\frac{r^2}{R_0^2}\right) \tag{18}$$

where $V(t)=V_z(t,r=0)$ is the velocity on the axis of the flow. Using (18) the term representing the viscous stresses effect in (6) can be rewritten as:

$$\frac{\mu}{\rho}\left(\frac{1}{r}\frac{\partial}{\partial r}\left(r\frac{\partial V_z\left(t,r\right)}{\partial r}\right)\right)=-\frac{4}{R_0^2}\frac{\mu}{\rho}\mathbf{V}\left(t\right) \tag{19}$$

Then with (6), (18) and (19), the velocity on the axis of the flow is given by:

$$\frac{d\mathbf{V}(t)}{dt}=\frac{Ed_{33}}{\rho Le}U(t)-\frac{1}{2L}k_{c\log}\mathbf{V}(t)^2-\frac{2\gamma}{\rho LR_0}-\frac{4}{R_0^2}\frac{\mu}{\rho}\mathbf{V}(t)$$

$$\Leftrightarrow\frac{\rho Le}{Ed_{33}}\dot{\mathbf{V}}=U-\frac{\rho e}{2Ed_{33}}k_{c\log}\mathbf{V}^2-\frac{2\gamma e}{Ed_{33}R_0}-\frac{4}{R_0^2}\frac{\mu Le}{Ed_{33}}\mathbf{V}$$

where

$$\dot{\mathbf{V}}=\frac{d\mathbf{V}\left(t\right)}{dt}.$$

The model used for the control synthesis is finally obtained:

$$\alpha\dot{\mathbf{V}}=U-\beta\,k_{c\log}\mathbf{V}^2-p-f_v\mathbf{V} \tag{20}$$

with :

$$\alpha=\frac{\rho Le}{Ed_{33}},\ \beta=\frac{\rho e}{2Ed_{33}}=\frac{\alpha}{2L},\ p=\frac{2\gamma e}{Ed_{33}R_0}=\frac{2\gamma\alpha}{\rho LR_0},$$

$$f_v=\frac{4\mu Le}{R_0^2Ed_{33}}=\frac{4\mu\alpha}{\rho R_0^2}.$$

For an industrial inkjet system we have the following constant: $\alpha\approx5^{10-5}$, $\beta\approx2$, $p\approx24.5$, $k_{clog}\geq0$.

The above constants are expressed in International System Units.

Experimentally, the flow velocity is only measured at the end of the first step of the ejection process. Moreover, the duration of the applied voltage step is such that the flow velocity reaches its final value. Thus, the main goal of the control system is to control the amplitude of the ejection velocity of the fluid, and to estimate and reject external perturbations caused by the clogging of the nozzle. Owing to the fact that the velocity is sampled at the end of the applied step voltage, and that at this time the velocity is constant (i.e. $\dot{\mathbf{V}}=0$), from (20) we obtain for the flow velocity at the end of the applied voltage:

$$\mathbf{V}\left(t=T_s\right)=\frac{1}{f_v}\left(U\left(t\right)-\beta\,k_{c\log}\mathbf{V}\left(t=T_s\right)^2-p\right) \tag{21}$$

where $U(t)=U_0$ and T_s are the amplitude and the duration of the applied voltage respectively, $t\in[0\ T_s]$.

Control System

We give below, in figure 5 a schematic of the control system including an estimation of the clogging effect:

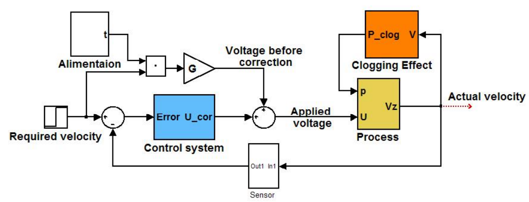

Figure 5. Control system using clogging estimation.

Figure 5 shows that the voltage is modified as a function of the tracking error.

Taking:

$$U_k=f_v\left(\mathbf{V}^*+z_k\right)+\beta\,\hat{k}_{c\log_k}\mathbf{V}^{*2}+p^* \tag{22}$$

where

$$z_k=z_{k-1}-K_ie_k \text{ and } \hat{k}_{c\log_k}=k_{c\log}=\frac{U_{k-1}-p-f_v\mathbf{V}_k}{\beta\mathbf{V}_k^{\ 2}}:$$

The system is stable for all $\hat{k}_{c\log_k}$ only if $K_i\in[0\ 2]$.

The control law based on the estimator performs much better that the integrator control law. So, if one assumes that the model is known, one can estimate the clogging level and control the process.

Figure 8 shows that if there is a perturbation on the output (velocity measurement in our case) the estimation is no more exact, but the system is still controlled.

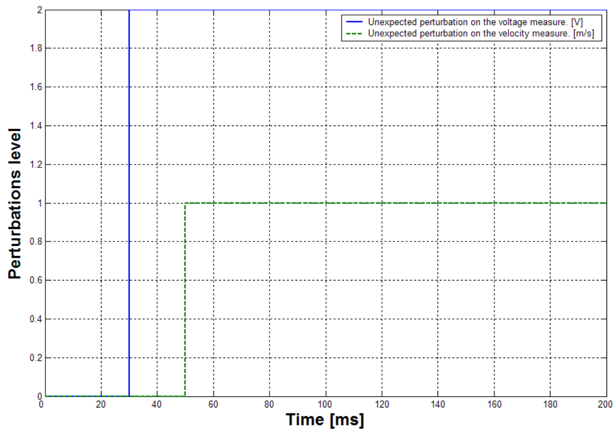

Figure 6. Transient evolution of the perturbation.

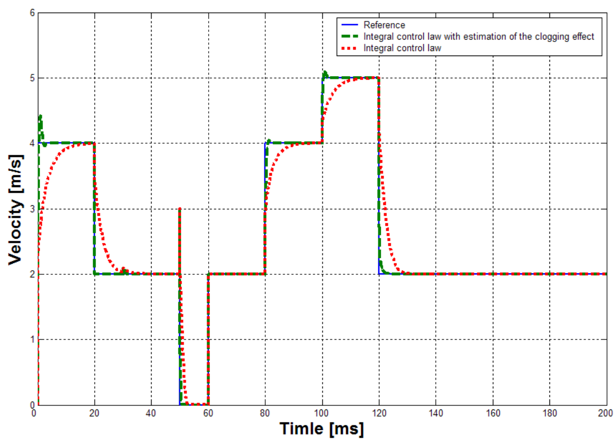

Figure 7. Comparison between two integral control law (with and without estimation)

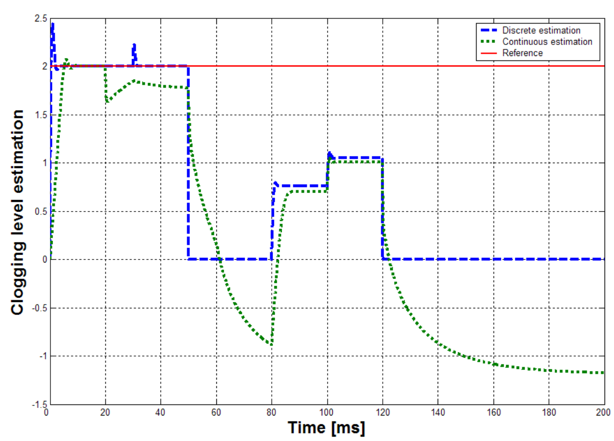

Figure 8. Clogging level estimation with unexpected perturbation.

Conclusion

In this paper, a simulation tool for piezoelectric micro-pumps is reported. Departing from the Navier-Stokes and piezoelectric equations for an axisymmetric configuration a generic model describing the functioning of piezoelectric micro-pumps is given. A second part focuses on the design of the control system and gives two control laws which are able to control and reject all perturbation on the system, or to control the system using the estimation of the nozzle clogging level. This work demonstrate that an adequate strategy can be found taking into account different operating condition. We will, in the future, work on the extension of the control system to multi-head printing processes.

Acknowledgement

The authors acknowledge financial support from the Région Rhône-Alpes through project 0201809702 and J.M.C. is particularly grateful to the Région Rhône-Alpes for a thesis funding. A.S. acknowledges support from the MNRT for partial funding of this project through Σ! 2911 PRODIJ. Finally, the authors wish to thank Guido Desie from Agfa-Gevaert Mortsel (Belgium) for allowing access to the experimental set-up.

References

1. F. G. Tseng, K. H. Lin, H. T. Hsu, and C. C. Chieng, Sens.Actuators A 111 (2004) 107-117.
2. S. C. Jakeway, A. J. de Melto, and E. L. Russel, J. Anal. Chem. 366 (2000) 525-539.
3. T. Kuroiwa, N. Ishikawa, D. Obara, F. Vinet, E.S. Ang, A. Guelbi, and A. Soucemarianadin, Proc. IS&T's NIP19: 2003 International Conference on Digital Printing Technologies, New Orleans, USA, 884-890.
4. D. C. Duffy, J. C. McDonald, O. J. A. Schueller, and G. M. Whitesides, Anal. Chem.,70 (1998) 4974-4984.
5. W. van der Wijngaart, H. Ask, P. Enoksson, and G. Stemme, Sens. Actuators A 100 (2002) 264-271.
6. H. Q. Li, D. C. Roberts, J. L. Steyn, K. T. Turner, O. Yaglioglu, N. W. Hagood, S. M. Spearing, and M. A. Schmidt, Sens. Actuators A 111 (2004) 51-56.
7. T. W. Shield, D. B. Bogy, and F. E. Talke, IBM J. Res Develop. Vol.31 No.1 January 1987.
8. JM. Cittadino, E. Mendes, and A. Soucemarianadin, Proc. IS&T's DPP'05: 2005 International Conference on Digital Printing applications, Amsterdam, Netherlands, 141-143.
9. PI Polytech: http://www.physikinstrumente.de/products/section4/content.php.
10. E. Guyon, J. P. Hulin and L. Petit, « Hydrodynamique Physique », InterEditions/Editions du CNRS, 1991.

Author Biography

J. M. Cittadino, 26 years old, is an engineer specialized in automatic control graduating from the National Polytechnic Institute of Grenoble (INPG). He is presently a final year doctoral student whose emphasis is on the design, modelling and optimisation of the control of microfluidic actuators.